Lipid Droplets Protect Human β-Cells From Lipotoxicity-Induced Stress and Cell Identity Changes

Xin Tong and Roland Stein

Diabetes 2021;70:2595–2607 | https://doi.org/10.2337/db21-0261

Free fatty acids (FFAs) are often stored in lipid droplet (LD) depots for eventual metabolic and/or synthetic use in many cell types, such a muscle, liver, and fat. In pancreatic islets, overt LD accumulation was detected in humans but not mice. LD buildup in islets was principally observed after roughly 11 years of age, increasing throughout adulthood under physiologic conditions, and also enriched in type 2 diabetes. To obtain insight into the role of LDs in human islet β-cell function, the levels of a key LD scaffold protein, perilipin 2 (PLIN2), were manipulated by lentiviral-mediated knockdown (KD) or overexpression (OE) in EndoCβH2-Cre cells, a human cell line with adult islet β-like properties. Glucose-stimulated insulin secretion was blunted in PLIN2KD cells and improved in PLIN2OE cells. An unbiased transcriptomic analysis revealed that limiting LD formation induced effectors of endoplasmic reticulum (ER) stress that compromised the expression of critical β-cell function and identity genes. These changes were essentially reversed by PLIN2OE or using the ER stress inhibitor, tauroursodeoxycholic acid. These results strongly suggest that LDs are essential for adult human islet β-cell activity by preserving FFA homeostasis.

Lipid droplet (LDs) are cellular organelles that typically play a key metabolic role by serving as a reservoir for cholesterol, acyl glycerol, and phospholipids used (for example) in signaling, energy homeostasis, and membrane maintenance (1). While the exposure of pancreatic islet α- and β-cells to excess lipids and glucose ultimately results in their dysfunction and type 2 diabetes (T2D) (2,3), it is very difficult to detect LDs in rodent islets even under obese, pathophysiological conditions where accumulation is evident in well-recognized, peripheral LD-storage cells in liver, muscle, and adipose tissue (4,5). Importantly, recent results suggest that LDs do accumulate in human islet α- and β-cells (5), which also differ from rodents with respect to islet cell composition, transcription factor (TF) expression, islet architecture, and glucose-stimulated insulin secretion (GSIS) (6–9).

Notably, LDs were found in human islet cells transplanted into immunocompromised mice raised on a normal or high-fat diet but not in similarly treated mouse islet cells (10). Strikingly, the compensatory mechanisms activated in response to the high-fat diet–induced insulin-resistant state were observed in transplanted mouse islets (e.g., elevated β-cell expansion and GSIS), while the non-responsive human islets accumulated LDs and islet amyloid plaques, the latter a hallmark of the T2D dysfunctional islet. The implication that LDs could impact islet cell function was further supported upon demonstration that LDs were in islet α- and β-cells within the intact human pancreas, with this most evident in post–juvenile age (>11 years) islet β-cells (5). Physiologic LD buildup was also found in the GSIS-responsive human embryonic stem cell–derived β-like cells produced in culture and after transplantation into immunocompromised mice. In contrast, LDs were very difficult to detect in the intact rodent pancreas under normal, aged, or pathophysiological conditions (5).

In addition, LDs were enriched in human T2D islet β-cells, which is possibly caused by the reduction in T2D-associated autophagic flux (5,11). We and others have proposed that human islet LDs serve to sequester toxic free fatty acids (FFAs) produced under insulin resistance conditions and that limitations in buildup and/or storage capacity result in islet β-cell dysfunction and elevated T2D susceptibility (10). However, the functional significance of LDs in human β-cells has not been delineated

Department of Molecular Physiology and Biophysics, Vanderbilt University, Nashville, TN

Corresponding author: Roland Stein, roland.stein@vanderbilt.edu

Received 26 March 2021 and accepted 19 August 2021

This article contains supplementary material online at https://doi.org/10.2337/figshare.15747093.

thoroughly, and to obtain such insight, we altered LD formation by reducing or overproducing the key LD scaffold protein PLIN2 in the adult human β-like cell line, EndoCβH2-Cre. Compromising LD production induced endoplasmic reticulum (ER) stress, reduced GSIS, and generated gene expression changes in cellular identity, which are all characteristics of T2D islet β cells (12–14). Furthermore, these lipotoxicity-induced changes were ameliorated by either elevating LD storage capacity by overexpressing PLIN2 or by pharmacological treatment with an ER stress inhibitor, tauroursodeoxycholic acid (TUDCA). These results strongly imply that LDs serve as a positive effector of adult human islet β-cell activity.

RESEARCH DESIGN AND METHODS

Human EndoCβH2-Cre Cells

EndoCβH2 cells were propagated in DMEM (Gibco and Thermo Fisher Scientific, Waltham, MA) in presence of 5.6 mmol/L glucose, 2% BSA (Serologicals Proteins, Kankakee, IL), 100 μU/mL penicillin, 100 μg/mL streptomycin, 50 μmol/L 2-mercaptoethanol, 10 mmol/L nicotinamide, 5 μg/mL transferrin, and 6.7 ng/mL sodium selenite (Sigma-Aldrich, St. Louis, MO) as previously described (15,16). Lentiviral vectors encoding shRNAs that were either scrambled (shScramble) (i.e., Sham) or to PLIN2 (shPLIN2) were constructed by VectorBuilder (Chicago, IL), as was the PLIN2 protein overexpressing cassette, with each containing a puromycin selection marker. The Cre-expressing lentivirus was made using the pTRIP ΔU3 CMV-nlsCre vector (17). Lentiviral particles were produced in human embryonic kidney 293T cells as previously described (18). Viral particles were isolated from the supernatant by either ultracentrifugation (18) or using the PEG-it Virus Precipitation Solution (System Biosciences, Mountain View, CA). The resultant pellets were resuspended in PBS or DMEM and aliquoted samples stored at −80°C. Viral particle amount was quantified with the Lenti-X p24 Rapid Titer Kit (Takara Bio, Mountain View, CA). EndoCβH2 cells were infected for 16 h with ∼50 ng shScramble, shPLIN2, or PLIN2 overexpression (OE) viral particles/million cells followed by puromycin selection; after that, all cells received the same viral dose of Cre expressing lentivirus for 18 days (16). The 10 mmol/L stock solution of palmitic acid (PA) (C16:0; Sigma-Aldrich) and erucic acid (EA) (C22:1; Sigma-Aldrich) was freshly prepared by dissolving in 90% ethanol followed by fatty acid–free BSA conjugation (Equitech-Bio, Inc.) in 0.01 mol/L NaOH solution at 55°C for 1 h, with a working concentration of 500 μmol/L for both. The 100 μmol/L TUDCA (Sigma-Aldrich) and N-acetyl-L-cysteine (Sigma-Aldrich) stocks were made in DMSO.

Immunofluorescence Analysis and LD Quantification

EndoCβH2-Cre cells cultured on chamber slides were fixed at room temperature for 12 min with 4% paraformaldehyde-PBS, permeabilized for 8 min with 0.5% Triton-PBS, and blocked for 30 min with 0.5% BSA-PBS followed by a 4°C overnight incubation with one of the following primary antibodies: anti-insulin (guinea pig, 1:500; Dako, Santa Clara, CA), anti-glucagon (mouse, 1:400; Sigma-Aldrich), anti-somatostatin (goat, 1:400; Santa Cruz Biotechnology, Santa Cruz, CA), anti-FEV (rabbit, 1:400; Thermo Fisher Scientific), anti-MAFA (rabbit, 1:500, cat. no. NBP1-00121; Novus), and anti-NKX2.2 (anti-goat, 1:400, Santa Cruz Biotechnology). Species-matched antibodies conjugated with the Cy2, Cy3, or Cy5 fluorophores were used for secondary detection (1:1,000; Jackson ImmunoResearch, West Grove, PA). BODIPY 493/503 (5 μmol/L in PBS; Thermo Fisher Scientific) was used to detect neutral lipid enriched LDs with incubation at room temperature for 30 min following the secondary antibody treatment. Images were acquired on a ZEISS Axio Imager M2 wide-field microscope with Apotome. Quantification of the LD level was calculated as the BODIPY 493/503 area divided by the $DAPI^+$ nuclear cell number with ImageJ software. Normalization was to the Sham control; at least five distinct areas of the slide from several independently generated sample sets were quantified per condition.

RNA Isolation, Reverse Transcription, and Real-time PCR

Total RNA was collected from EndoCβH2-Cre cells using the Trizol reagent (Life Technologies) in accord with the manufacturer's instructions. The iScript cDNA synthesis kit (Bio-Rad Laboratories) was used for cDNA synthesis. Quantitative real-time PCR reactions were performed with the primers described in Supplementary Table 1 on a LightCycler 480 Instrument II (Roche) and analyzed by the ΔΔCT method. Significance was calculated by comparing the ΔCT values.

Bulk RNA-Sequencing Analysis

The RNeasy Plus Mini Kit (QIAGEN) was used to isolate total RNA from treated EndoCβH2-Cre cells ($n = 3$) and RNA quality control analyzed on an Agilent 2100 Bioanalyzer. Only samples with an RNA Integrity Number >8.0 were used for library preparation. cDNA libraries were constructed and paired-end sequencing was performed on an Illumina NovaSeq 6000 (150 nucleotide reads). The generated FASTQ files were processed and interpreted with the Genialis visual informatics platform (https://www.genialis.com) (15). Sequence quality checks were performed with use of raw and trimmed reads with FastQC (https://www.bioinformatics.babraham.ac.uk/projects/fastqc), and Trimmomatic was used to trim adapters and filter out poor-quality reads. Trimmed reads were then mapped to the University of California, Santa Cruz, hg19 reference genome with use of the HISAT2 aligner. Gene expression levels were quantified for htseq-count and differential gene expression analyses performed with DESeq2. All detectable genes were included in the pathway analysis (Kyoto Encyclopedia of Genes and Genomes [KEGG] and Gene Ontology [GO] term) as part of the Enrichr bioinformatics analysis

platform (https://maayanlab.cloud/Enrichr/) to prevent bias. Some of the heat map selected genes were manually curated based on Gene Set Enrichment Analysis (GESA) (https://www.gsea-msigdb.org/gsea/index.jsp) and published gene or RNA-seq data sets (19–21).

However, poorly expressed genes, which had average expression count in all samples of <5 transcripts per million (TPM), were filtered out of the gene lists and heat maps.

Static GSIS

Static insulin secretion was assessed as previously described (22) in EndoCβH2-Cre cells, which involved a 1-h incubation at 37°C in 2.5 mmol/L glucose secretion assay buffer, and then with freshly prepared 2.5 or 16.7 mmol/L glucose secretion assay buffer for another hour. The outcome was presented as the secreted insulin (Lumit Insulin Immunoassay, Promega, and human insulin ELISA, Crystal Chem) relative to the total insulin content. The secreted insulin data were normalized to basal secretion of the Sham at 2.5 mmol/L glucose. Insulin content was presented as the concentration of insulin normalized to total DNA content (Quant-iT PicoGreen; Invitrogen) in each condition (ng/ng DNA) relative to the Sham. At least three independently generated sets of samples were analyzed under each condition.

Immunoblot Analysis

Whole cell protein extracts were prepared from EndoCβH2-Cre cells using radioimmunoprecipitation assay buffer (Sigma-Aldrich) containing a cocktail of protease and phosphatase inhibitors (Roche Applied Science). The extracted proteins (15 ng) were resolved on a 4–20% Mini-PROTEAN (Bio-Rad Laboratories) electrophoresis gel and immunoblotted with anti–spliced XBP-1 and anti-actin antibodies (Proteintech and MilliporeSigma, respectively) (Supplementary Table 1). The densitometry of the protein bands was calculated with ImageJ software.

Statistical Analysis

Significance was determined with the two-tailed Student *t* test. Data are presented as the mean ± SD. A threshold of $P < 0.05$ was considered significant.

Data and Resource Availability

The data sets generated during or analyzed during the current study are available from the corresponding author. The bulk RNA-seq data set have been uploaded to Gene Expression Omnibus (GEO) with the accession #GSE184016.

RESULTS

PLIN2 Regulates LD Levels in EndoCβH2-Cre β-Cells

To obtain insight into the functional role of LDs in human β-cells, the mRNA levels of core structural perilipins were first determined in proliferating EndoCβH2 and nonproliferating EndoCβH2-Cre cells. Lentiviral-mediated Cre treatment and its expression in EndoCβH2 cells remove the endogenous floxed SV40 virus Tag transforming protein to prevent cell proliferation and allow functional maturation (Fig. 1*A*). The resulting EndoCβH2-Cre cell line produces high insulin levels and adult islet β-like GSIS responsivity (16). PLIN2 was the principal member of the gene family produced in human and mouse islets (5,23) (Fig. 1*B*). Cells were infected with lentivirus expressing shPLIN2 or PLIN2 cDNA to knockdown (KD) or overexpress (OE) PLIN2, with these conditions reducing mRNA levels by roughly 70% or inducing by about 50% (Fig. 1*C*). PLIN2KD and PLIN2OE treatment did not influence the expression of other PLINs (Fig. 1*C*) and had no impact on cell proliferation, cell death, or cell morphology state of EndoCβH2 or EndoCβH2-Cre cells (data not shown). PLIN2 mRNA levels were elevated upon inducing GSIS in EndoCβH2-Cre cells (Fig. 1*B*), a property also observed in rodent β-cell lines (24).

The impact of PLIN2KD and PLIN2OE on LD accumulation was evaluated in EndoCβH2-Cre cells treated with two FFAs, PA (C16:0) or EA (C22:1). PA induces a much milder cell stress response in relation to EA in EndoCβ1H cells (25), a closely related human β-cell line. As expected from studies in other contexts (26), BODIPY 493/503–detected LD accumulation was decreased significantly following PLIN2KD treatment and enhanced by PLIN2OE (Fig. 1*D* and *E*). Because of the higher toxicity profile of EA than PA in EndoCβ1H (25), EA was the FFA of choice to study lipotoxicity in our EndoCβH2-Cre experiments.

PLIN2 Level Regulates Insulin Secretion

PLIN2KD prevented GSIS in EndoCβH2-Cre cells (Fig. 2*A*), while PLIN2OE may enhance in comparison with the Sham. The loss of GSIS was not due to reduced insulin mRNA production in PLIN2KD or a difference in insulin protein levels between PLIN2KD and PLIN2OE cells (Fig. 2*B* and *C*).

Bulk RNA-sequencing (RNA-seq) analysis performed on Sham, PLIN2KD, and PLIN2OE EndoCβH2-Cre cells revealed that a large number of positive effectors of insulin secretion were impacted upon PLIN2/LD manipulation. Not surprisingly, expression of these were reduced in PLIN2KD and boosted by PLIN2OE (Fig. 2*D*). These differences were also verified upon quantitative PCR analysis of various regulatory candidates (Fig. 2*E*), including *EXOC5* (27), which is involved in vesicle docking and fusion; *KCNJ11* (28) encoding the ATP-sensitive inward rectifier potassium channel 11; *SNAP 25* (29) of the SNARE complex; and *STX1A* (14), which is important in vesicle membrane docking. Taken together, our data suggest that LD accumulation affects the insulin secretory machinery and GSIS in human β-cells.

PLIN2KD Induces ER Stress and Compromises Ca^{2+} Homeostasis Gene Expression

The RNA-seq results revealed that PLIN2KD in EndoCβH2-Cre cells had 1,479 upregulated and 493 downregulated genes compared with Sham, while 237 were elevated and 48 decreased in PLIN2OE cells (Supplementary Tables 2 and 3

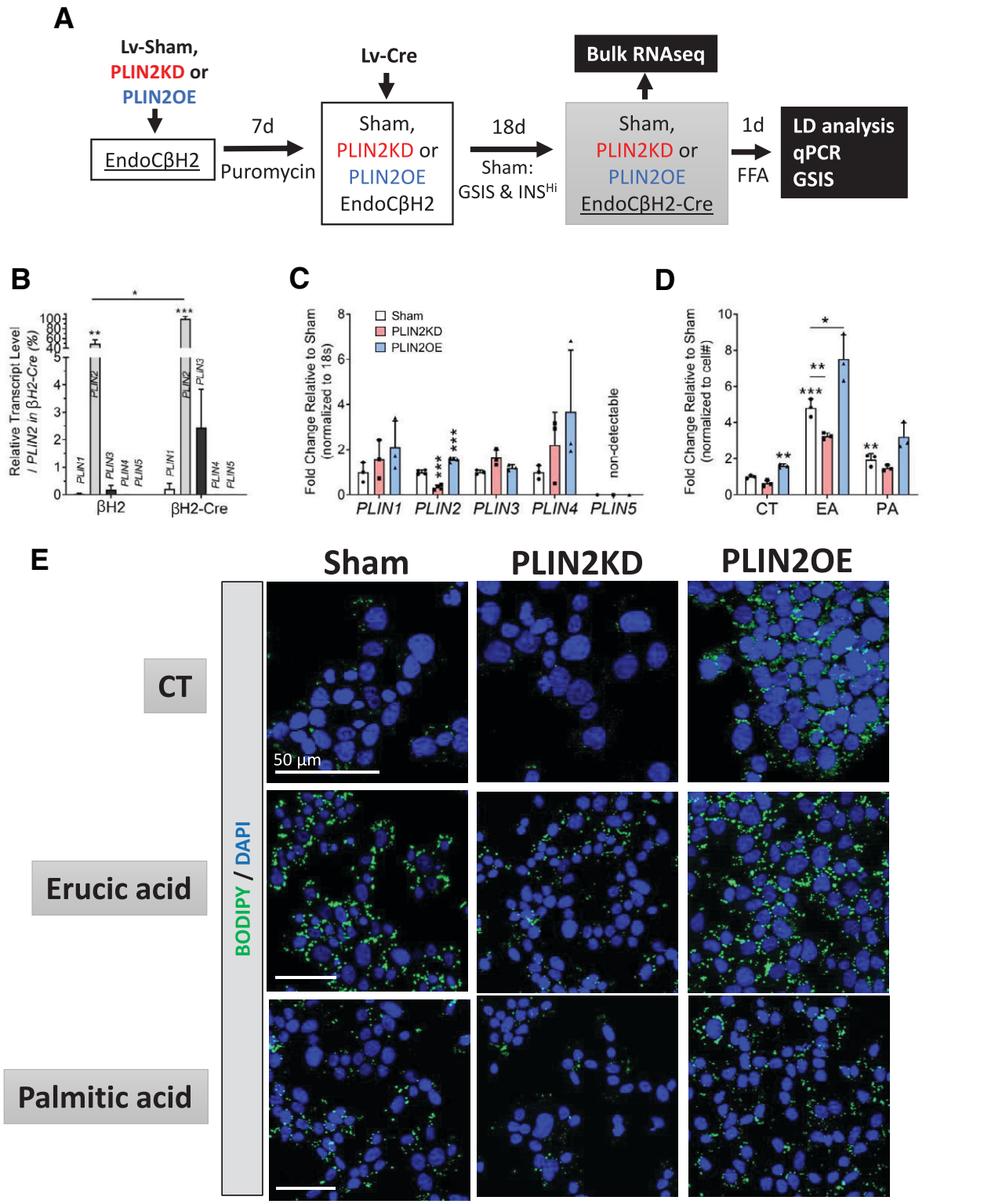

Figure 1—PLIN2 influences LD accumulation in human EndoCβH2-Cre β-cells. *A*: Experimental workflow and depiction of how maturation changes upon Cre-mediated SV40 Tag removal. *B*: The expression level of all members of the PLIN family before and after Cre treatment. Both *PLIN2* and *PLIN3* levels increased significantly. *C*: The change in *PLIN* mRNA levels upon PLIN2KD and PLIN2OE. *D*: Quantitation of the change in LD levels between Sham and PLIN2KD or PLIN2OE cells incubated without (control [CT]) or with 500 μmol/L EA or PA for 24 h. *E*: Representative images of *D*. Notably, FFA-induced LD accumulation appears to positively correlate with PLIN2 levels, which was statistically significant in the EA-treated group. All error bars indicate SD. $n = 3$–4. *$P < 0.05$, **$P < 0.01$, ***$P < 0.05$ vs. βH2 or βH2-Cre PLIN1 (*B*), Sham (*C*), or control (*D*) unless specified. βH2, EndoCβH2; βH2-Cre, EndoCβH2-Cre; Lv, lentivirus; qPCR, quantitative PCR.

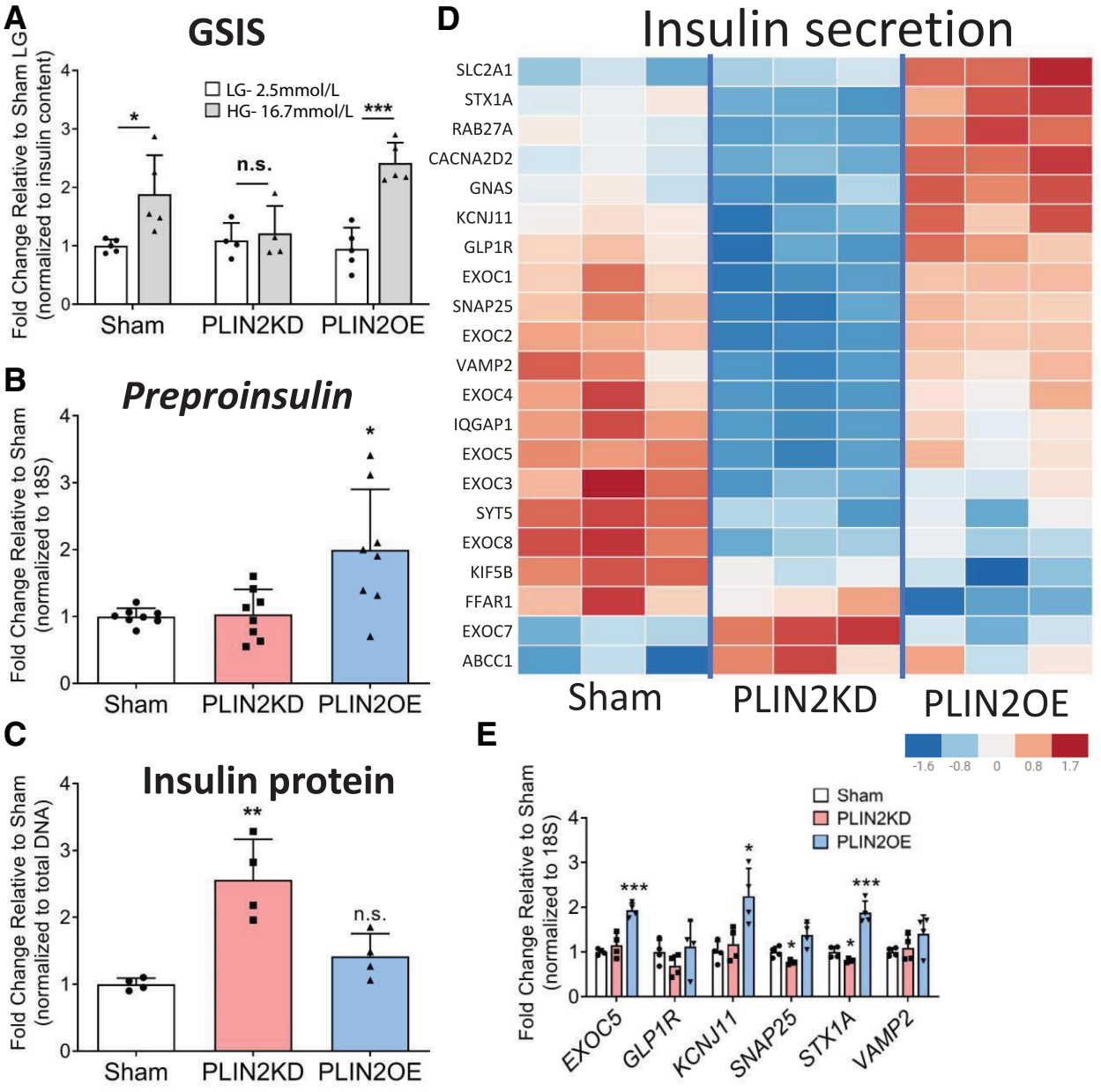

Figure 2—PLIN2/LDs regulate GSIS in EndoβCH2-Cre cells. *A*: GSIS was blocked in PLIN2KD cells compared with Sham, whereas this was enhanced in PLIN2OE. Levels were first normalized to DNA content and then to Sham at 2.5 mmol/L glucose. Preproinsulin mRNA (*B*) trended higher in both PLIN2OE and PLIN2KD cells, although insulin protein levels (*C*) were only elevated in PLIN2KD. Normalization was to 18S (*B*) or DNA content (*C*) before Sham. *D*: The heat map shows that insulin secretion–related gene expression was generally decreased in PLIN2KD cells, while it was elevated in PLIN2OE cells. The color keys represent the row-wise *Z* score. False discovery rate < 0.05. *E*: Quantitative real-time PCR analysis of selected secretory gene changes. All error bars indicate SD. $n = 3$–8. *$P < 0.05$, **$P < 0.01$, ***$P < 0.001$ vs. corresponding LG (*A*) or Sham (*B*–*E*). HG, high glucose; LG, low glucose; n.s., nonsignificant.

provide the full list of differentially expressed genes [i.e., DEGs]). We next focused on obtaining a more thorough understanding of why reducing LD accumulation eliminated GSIS (Fig. 2*A*). KEGG and GO (GO term) analysis revealed that the PLIN2KD cells manifested gene expression profiles characteristic of proinflammatory cytokine treatment and glucolipotoxicity (19) (Supplementary Table 4). For example, the positively affected "AGE-RAGE signaling in diabetic

complications" and "inflammation-like" pathways mediate proinflammatory signaling and ER stress in other systems (30), while β-cell dysfunction would also have resulted upon downregulating proteins essential to pathways associated with "insulin secretion," "cAMP signaling," "maturity onset diabetes of the young," "voltage-gated cation channel activity," "gap junction channel activity," and "cytoskeleton molecule binding."

In contrast, while the PLIN2OE cells more closely resembled the Sham, KEGG analysis revealed DEGs predicted to enhance β-cell activity, including elevating "gap junction activity" and "microtubule motor activity," as well as reducing "TNF signaling" and "cytokine/chemokine activity" pathway gene encoded proteins (Supplementary Table 5). Importantly, these properties are opposite those of PLIN2KD cells (Supplementary Table 4). In addition, genes important in "transforming growth factor β (TGFβ) receptor signaling," a pathway negatively regulating β-cell function and identity (31), were only elevated upon PLIN2KD (Supplementary Fig. 1).

For counteraction of ER stress conditions that can result in β-cell death, three arms of a network of signaling pathways may be activated to restore ER homeostasis: *1*) ATF6, *2*) IRE1α-XBP1, and *3*) PERK-eIF2α, which collectively orchestrate the selective transcription and translation of ER chaperones, and elimination of misfolded proteins by ER-associated degradation and autophagy, and reduce incoming protein load by decreasing global transcription and translation (32). Our RNA-seq and qPCR results indicate that the IRE1α-XBP1 pathway was primarily activated in PLIN2KD EndoCβH2-Cre cells and not the ATF4/6 (i.e., which leads to CHOP activation) or PERK (Fig. 3*A* and *B*) pathway. Elevated spliced (s)XBP1 protein levels were also found in the PLIN2KD (Fig. 3*C*). In addition, many ER regulators essential to Ca^{2+} homeostasis and insulin secretion in islet β-cells were mis-regulated in PLIN2KD cells (e.g., Fig. 3*D*), an effect that would contribute to blunting the GSIS response (33). Significantly, many genes involved in these pathways were among the most upregulated in PLIN2KD cells (Supplementary Table 6) (e.g., *ERN1* [IRE1α], *DDIT4* [CHOP], *TGFB2*, and *BMP2*). On the contrary, a key TGFβ signaling regulatory gene was downregulated in PLIN2OE cells (Supplementary Table 7) (*SMAD7*).

PLIN2KD Influences β-Cell Identity

Cellular stress is believed to be a driver of T2D islet cell dysfunction and loss of β-cell identity (12,13), which is manifested by decreased expression of essential TF genes, mis-expression of nonislet β hormones, induced production of gene products incompatible with adult function (i.e., termed the disallowed genes [21]), and the synthesis of progenitor/dedifferentiation markers (34). Strikingly, these same characteristics were witnessed upon simply reducing LD accumulation in PLIN2KD EndoCβH2-Cre cells (Fig. 4*A* and *B*), as exhibited, for example, by increased gene production levels of non–β-cell POMC, SST, and NPY hormones; elevated islet progenitor FEV, FOS, and SOX9 TF markers; mis-expression of disallowed genes; and reduced expression of islet-enriched MAFA, NKX2.2, PDX1, and NKX6.1 TF genes. However, none of these changes were observed in PLIN2OE cells (Fig. 4*B*, data not shown). Interestingly, immunostaining revealed that only a fraction of PLIN2KD EndoCβH2-Cre cells produced the α-cell glucagon and δ-cell somatostatin hormones (Fig. 5*A*) or the FEV protein (35) that is normally principally produced in the Neurogenin 3^{+} TF islet progenitor cell population (Fig. 5*B*). In contrast, islet cell–enriched MAFA and NKX2.2 TF levels appeared to be decreased throughout the β-cell population (Fig. 5*D*). As expected, PLIN2OE prevented these changes found upon PLIN2KD (Fig. 5). Collectively, these results imply that LD accumulation regulates both the cell identity and function of human islet β-cells.

ER Stress Is an Important Effector of PLIN2KD-Induced Dysfunction

Given the pronounced elevation in multiple markers of ER stress in PLIN2KD EndoCβH2-Cre cells, a bile acid analog commonly used to inhibit this response, TUDCA, was tested in this context. The effects of PLIN2KD on GSIS (Fig. 6*A*) and insulin levels (Fig. 6*B*) were reversed by TUDCA treatment, with levels now indistinguishable from those of Sham. As anticipated from these results, the expression of a representative panel of genes that affected insulin secretion, ER stress, islet TFs, and progenitor/identity almost returned to Sham-like levels after TUDCA treatment of PLIN2KD cells (Fig. 6*C*). In contrast, a general oxidative stress inhibitor, N-acetyl cysteine, appears to have further compromised PLIN2KD cells (Supplementary Fig. 2). Notably, those genes influenced to a lesser extent by TUDCA were produced in a small subfraction of the β-cell population (e.g., FEV [Fig. 5*B*] and likely the HHEX [36] TF of the somatostatin gene). Moreover, treatment with EA negatively impacted GSIS as well as induced ER stress–responsive and progenitor/identity gene expression, all of which were virtually blunted by PLIN2OE (Fig. 6*A*–*C*).

sXBP1 protein levels were also elevated in PLIN2KD cells and not by PLIN2OE treatment (Fig. 6*D*). However, Sham sXBP1 protein levels were slightly decreased by EA in the context of elevated mRNA expression (see Fig. 6*C* and *D*), implying that insufficient LD production regulates sXBP1 synthesis/accumulation and ER stress in human β cells. Notably, EA also induced a much more robust stress response than PA in EndoCβH2-Cre cells (Supplementary Fig. 3), as originally described in EndoCβH1 cells (25). In total, our data strongly indicate that LDs are beneficial to human islet β cells, with our mechanistic analysis implying that their ability to sequester toxic FFA prevents ER stress, loss of cell activity, changes in cell identity, and decreased cell health (Fig. 7).

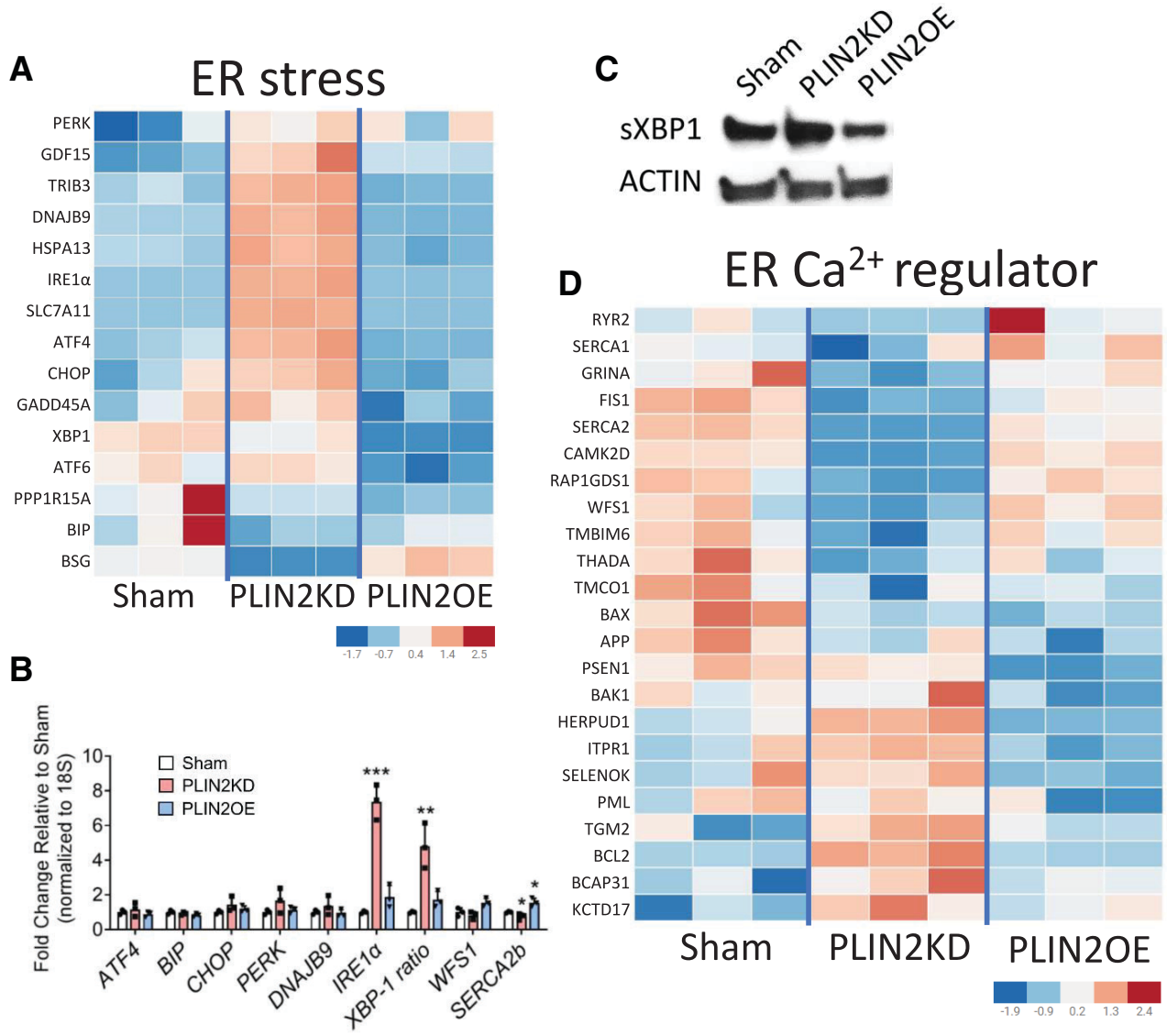

Figure 3—PLIN2KD induces ER stress. Heat maps showing how PLIN2KD influences the expression of genes involved in ER stress (*A*) and ER Ca^{2+} homeostasis (*D*). The color keys represent the row-wise *Z* score. *B*: Quantitative real-time PCR analysis of selected ER stress and ER Ca^{2+} regulators from panels *A* and *D*. *C*: A representative immunoblot of sXBP1 and ACTIN protein levels in Sham, PLIN2KD, and PLIN2OE cells. All error bars indicate SD. $n = 3$. *$P < 0.05$, **$P < 0.01$, ***$P < 0.001$ vs. Sham.

DISCUSSION

The functional role of LDs in cells has been studied extensively under both healthy and diseased conditions in many contexts, including in muscle, liver, and adipose tissues (1). The general consensus has been that LDs normally serve as a storage depot for neutral lipids and cholesterol for anabolic and catabolic needs, with lipotoxicity produced under pathological conditions due (at least in part) to limitations in FFA storage and/or breakdown in LDs (4). In contrast, studies in mice suggest that LD accumulation is detrimental to islet β-cell health, since whole-body PLIN2 knockout in mice or KD of PLIN2 in rodent β-cell lines has improved autophagic flux, reduced ER stress, and decreased β-cell apoptosis (24,37). However, we and others have found that LDs are very difficult to find in the rodent pancreas, whereas they are readily detected in adult humans and are even enriched in T2D islets (5,11). Because human and rodent islets differ substantially in architecture, cell composition, proliferative capacity, islet amyloid formation, and antioxidant enzyme levels (7,10,38,39), the EndoCβH2-Cre cell line was used to examine the influence of LDs in human β-cells, a well-established model system whose molecular composition and GSIS properties are quite similar to those of adult islet β-cells (16,40). Our data strongly suggest that LDs function, in part, to insulate human β-cells from noxious

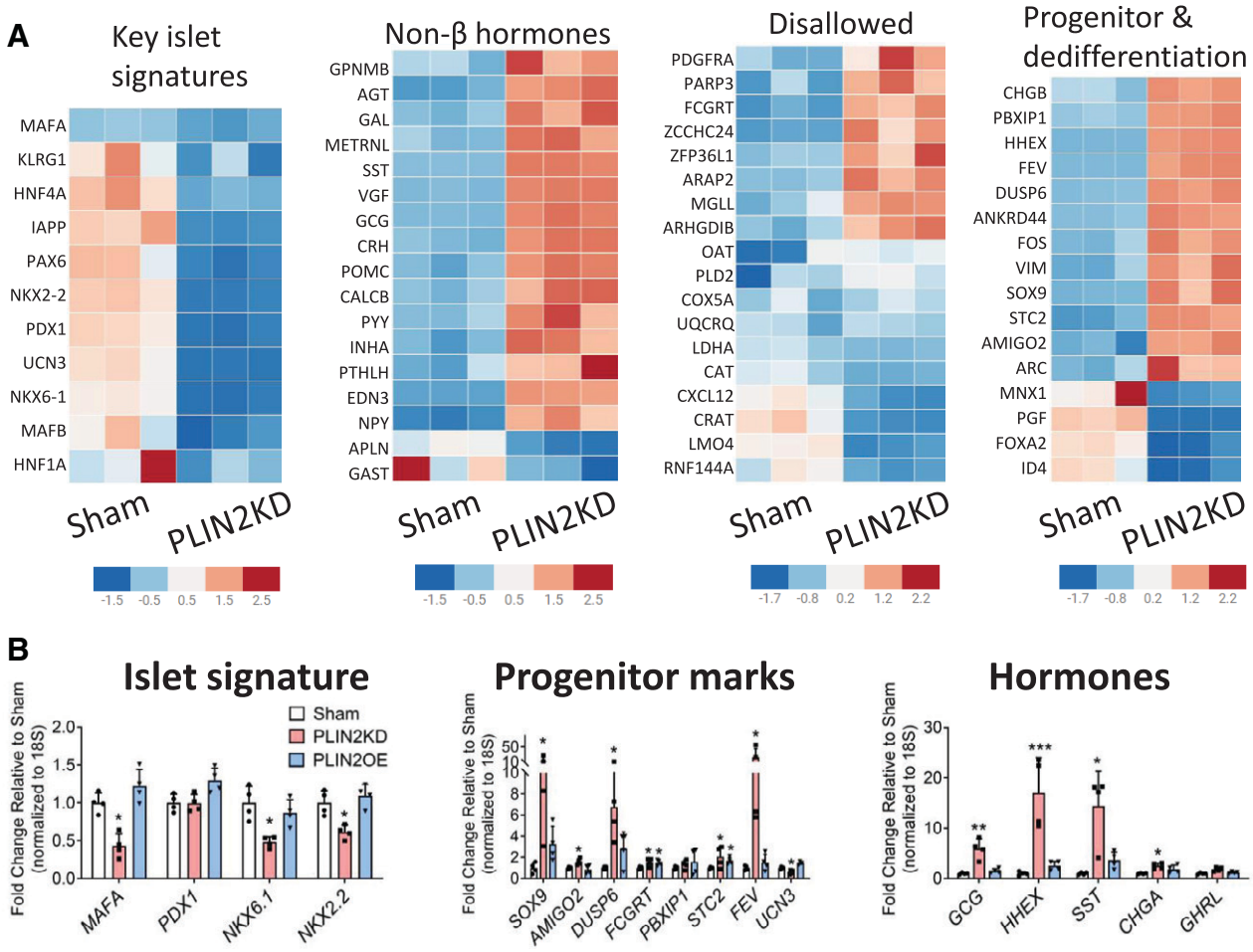

Figure 4—PLIN2KD influences β-cell identity. *A*: Heat maps illustrating the changes in PLIN2KD cells in expression of key β-cell signature genes, non–β-cell hormone genes, disallowed genes, and genes enriched in embryonic progenitors and dedifferentiated β-cells. The color keys represent the row-wise *Z* score. *B*: Quantitative real-time PCR results of candidates in Sham, PLIN2KD, and PLIN2OE cells. All error bars indicate SD. $n = 3$–4. *$P < 0.05$, **$P < 0.01$, ***$P < 0.001$ vs. Sham.

FFA exposure until a threshold capacity for LDs is reached, after which these cells are vulnerable to lipotoxicity-induced ER stress, dysfunction, loss of identity, and overall compromised cell health (Fig. 7). Consequently, differences in LD formation and/or degradation could be a contributing factor to T2D islet β-cell dysfunction.

Limiting LD Accumulation Induces Lipotoxic-Like ER Stress and Dysfunction

Manipulating PLIN2 levels significantly altered LD accumulation levels in EndoCβH2-Cre cells (Fig. 1*D* and *E*), a result consistent with many studies showing that LD formation is dependent on perilipin structural protein levels (23). This resulted in the reduction in GSIS in PLIN2KD cells and a trend towards improvement by PLIN2OE (Fig. 2*A*). RNA-seq analysis suggested that limiting LD formation induced IRE1α-activated ER stress, which reduced production of a variety of effectors of insulin secretion. This included not only the expression of mRNA encoding proteins directly involved in this process (Fig. 2*D* and *E*) but also critical mediators and signaling pathways regulating GSIS (e.g., ER Ca^{2+} [Fig. 3*B*] and TGFβ [Supplementary Fig. 1]). These results are not consistent with those of earlier work in rodents (24,37), yet they are with recent findings in rat INS-1 β-cells and human islets (41). Although this newer work had only limited molecular detail in how compromising LD formation negatively impacted β-cell function, their physiological results showed that mitochondrial health and activity were negatively impacted in both rodent β-cells and human islets (41). Notably, our RNA-seq data also suggest that the integrity of PLIN2KD mitochondria is compromised (Supplementary Fig. 4).

Our results suggest that ER stress facilitates lipotoxicity in human β-cells with limited LD storage capacity (Figs. 3 and 6). Indeed, cellular stress appears to be a mediator of this condition in many tissues (42). For example, LDs were generated in mouse embryonic fibroblasts to protect against mitochondrial dysfunction induced upon FFA release from autophagic degradation of membranous organelles, a

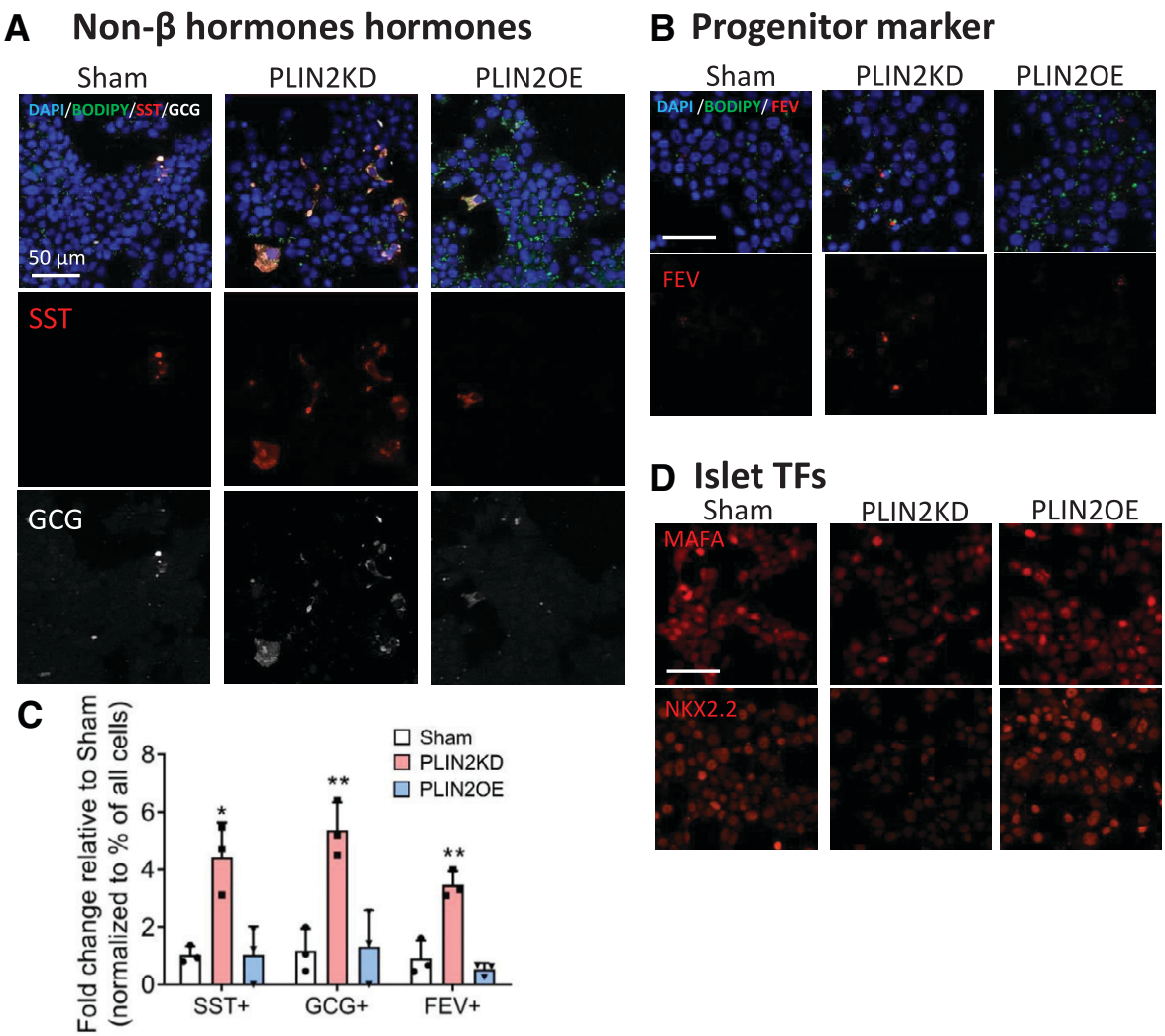

Figure 5—Cellular distribution of proteins linked to β-cell identity in PLIN2KD cells. Immunofluorescent staining illustrates that somatostatin (SST) (red) and glucagon (GCG) (white) (*A*) and FEV (red) (*B*) protein production is only found in a small fraction of PLIN2KD cells, with quantitation of the change in SST^+, GCG^+, or FEV^+ cell percentages between Sham and PLIN2KD or PLIN2OE cells (*C*); all error bars indicate SD. $n = 3$. $^*P < 0.05$, $^{**}P < 0.01$ vs. Sham. *D*: In contrast, MAFA (red, top panel) and NKX2.2 (red) protein levels were lower in most PLIN2KD cells. The remaining $MAFA^+$ and $NKX2.2^+$ cells in the PLIN2KD population probably represent uninfected cells. DAPI (blue) and BODIPY (green) counterstaining. Scale bar = 50 μm.

diacylglycerol acyltransferase 1–dependent process. This enzyme, which catalyzes the terminal step in triacylglycerol synthesis, is also necessary in preventing ER stress during adipose tissue inflammation (43). In addition, reducing LD formation or storage capacity (e.g., by OE of the lipolysis enzyme adipose triglyceride lipase) results in the generation of proinflammatory and ER stress markers in liver and cardiomyocytes (44,45), while improving LD levels by perilipin protein OE lowered their levels in skeletal muscle (46). The overall protective role of LDs in preventing stress was also observed in many cancer cells during metastasis (47).

LD Maintenance Is Essential for Sustaining β-Cell Identity

The loss of islet β-cell identity produced by glucolipotoxicity-induced ER stress (48) is a characteristic of T2D islets (12,13), as manifested by fewer $insulin^+$ cells, limited islet enriched TF gene expression, induction of disallowed gene production, and gain in nonislet β-cell hormone synthesis. Significantly, these same properties were observed in PLIN2KD EndoCβH2-Cre cells (Fig. 4). Moreover, changing perilipin levels also influenced adipose cell identity, with PLIN2 deletion or PLIN1 OE promoting the browning of white adipose tissue (49).

Here we observed that MAFA and NKX2.2 protein levels were dysregulated throughout the PLIN2KD cell population, while glucagon, somatostatin, and FEV were only produced in a small fraction (Fig. 5). This may represent the temporal progression of T2D, with prediabetes broadly inducing limitations in islet β-cell function that become more severe over time and eventually result in a reduction in insulin levels and gaining (for example) non–β-cell hormone and progenitor cell marker production. However, we did not

Figure 6—TUDCA rescues PLIN2KD-induced dysfunction, while PLIN2OE prevents EA toxicity. Sham, PLIN2KD, and PLIN2OE cells were treated with TUDCA (100 μmol/L) and/or EA (500 μmol/L) for 24 h. The toxic effects of PLIN2KD and EA on GSIS (*A*) and insulin levels (*B*) were rescued by TUDCA and PLIN2OE treatment, respectively. *C*: Expression of the majority of candidate regulatory genes was corrected to Sham by TUDCA or PLIN2OE. Ins, insulin. *D*: On the left is a representative immunoblot and on the right the quantification of multiple sXBP1 and ACTIN analyses performed on Sham, PLIN2KD, and PLIN2OE cells. All error bars indicate SD. $n = 3$–4. $^{*}P < 0.05$, $^{**}P < 0.01$, $^{***}P < 0.001$ vs. corresponding LG (*A*) or Sham (*B*–*D*) unless specified. ET, erucic acid + TUDCA; HG, high glucose; LG, low glucose; n.s., nonsignificant.

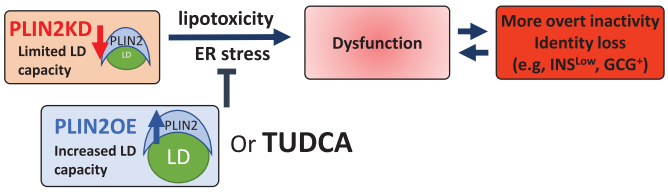

Figure 7—Model illustrating the proposed importance of FFA storage in LDs to human β-cell health.

observe induction of the very early islet cell progenitor signatures first observed upon FoxO1 TF β-cell deficiency in mice, like Nanog, Neurogenin 3, Oct4, and L-Myc (34). Notably, these markers are not a feature in all human T2D studies (50), which may reflect the heterogeneity of the disease and/or methodological differences (51). Progenitor cell marker expression in PLIN2KD cells was represented by FEV, which is normally expressed at high levels in islet Neurogenin 3^+ progenitors developmentally as well as later at lower levels in immature insulin$^+$ cells and adult islet β-cells (35). FEV levels are also elevated in T2D islets (52). It is presently unclear whether bona fide markers of dedifferentiation, like Neurogenin 3, are simply not regulated by LD/lipotoxicity levels in human β-cells or represent a limitation of the conditions and/or model used for experimentation.

There Appear to Be Many Similarities in the Signaling Pathways Regulated by Lipotoxicity and PLIN2KD in Human β-Cells

As hoped of the human PLIN2KD model, there were many differentially regulated genes shared with palmitate-treated human islets (19). These included genes controlling ER stress, extracellular matrix, and metabolic signaling pathways (Supplementary Fig. 5). As dyslipidemia is one of the highest T2D risk factors (53), it was also not surprising that there was overlap between PLIN2KD and T2D islet dysregulated genes (Supplementary Fig. 6*A*). In addition, overlap was found with T2D-associated genes/pathways found in genome-wide association studies (Supplementary Tables 2 and 4 and Supplementary Fig. 6*B*), including an FFA desaturase found to maintain n-6 and n-3 polyunsaturated fatty acid level and the proinflammatory phenotype in liver (i.e., *FADS1*), a G protein–coupled receptor for medium- and long-chain unsaturated fatty acids that protects against lipotoxicity-induced pancreatic β-cell dysfunction (*GPR120*), and a master lipid TF regulator that plays a role in β-cell function (*PPARγ* [54]). In addition, a number of PLIN2KD DEGs (108 of 1,972) overlapped with genes critical to FFA uptake, lipid synthesis, breakdown, and storage (Supplementary Fig. 7). This evidence supports a strong relationship between FFA and LD homeostasis in human β-cell function and health. Furthermore, many amino acid metabolism-related genes altered in PLIN2KD cells are changed in individuals with T2D (55) (i.e., in the "Glycine, serine, threonine, cysteine and methionine metabolism" pathway [Supplementary Table 4]).

While the positive impact on GSIS of either TUDCA or PLIN2OE treatment on EndoCβH2-Cre cells strongly indicates that ER stress is a primary driver of lipotoxicity in human islet β-cells (Figs. 3 and 6), precisely how limiting LD formation leads to dysfunction is still unclear. For example, could other critical signaling molecules bind to this organelle, which, for example, involves proteasomal components and TFs first found in hepatocytes (56,57)? Future studies should also determine whether acute changes in LD levels influence adult human islet β-cells differently than EndoCβH2-Cre cells, and whether accumulation affects transplanted islet human islet β-cell function in vivo, which are unable to mount the proliferation or secretion response of mouse β-cells needed to compensate for the insulin-resistant state imparted by high-fat diet–induced stressors (10). Thus, we believe it is important to determine how LD levels impact islet cell vulnerability to lipotoxicity, presuming that these processes influence T2D susceptibility. Importantly, this study supports such efforts by providing a linkage between LD homeostasis and human β-cell integrity.

Acknowledgments. The authors thank Drs. Raphaël Scharfmann from Institute Pasteur, Paris, France, and Phillippe Ravassard from French National Centre for Scientific Research, Paris, France, for generously providing EndoCβH2 cells, Dr. Rotonya Carr from University of Pennsylvania for intellectual guidance, Dr. Jinhua Liu from Vanderbilt University for experimental assistance, and Dr. Jeeyeon Cha from Vanderbilt University Medical Center for reading and editing the manuscript.

Funding. This research was performed using resources or funding provided by National Institute of Diabetes and Digestive and Kidney Diseases, National Institutes of Health, grants to R.S. (DK090570, DK050203, DK126482) and the Vanderbilt Diabetes Research and Training Center (DK20593). X.T. was supported by a JDRF fellowship (3-PDF-2019-738-A-N).

Duality of Interest. No potential conflicts of interest relevant to this article were reported.

Author Contributions. X.T. and R.S. designed the experiments. X.T. executed and analyzed the experiments with input from R.S. The manuscript was written by X.T. and R.S. R.S. is the guarantor of this work and, as such, had full access to all the data in the study and takes responsibility for the integrity of the data and the accuracy of the data analysis.

References

1. Walther TC, Farese RV. Lipid droplets and cellular lipid metabolism. Annu Rev Biochem 2012; 81:687–714

2. Poitout V, Amyot J, Semache M, Zarrouki B, Hagman D, Fontés G. Glucolipotoxicity of the pancreatic beta cell. Biochim Biophys Acta 2010;1801:289–298

3. Kumar B, Kowluru A, Kowluru RA. Lipotoxicity augments glucotoxicity-induced mitochondrial damage in the development of diabetic retinopathy. Invest Ophthalmol Vis Sci 2015;56:2985–2992
4. Onal G, Kutlu O, Gozuacik D, Dokmeci Emre S. Lipid droplets in health and disease. Lipids Health Dis 2017;16:128
5. Tong X, Dai C, Walker JT, et al. Lipid droplet accumulation in human pancreatic islets is dependent on both donor age and health. Diabetes 2020;69:342–354
6. Rodriguez-Diaz R, Abdulreda MH, Formoso AL, et al. Innervation patterns of autonomic axons in the human endocrine pancreas. Cell Metab 2011;14:45–54
7. Brissova M, Fowler MJ, Nicholson WE, et al. Assessment of human pancreatic islet architecture and composition by laser scanning confocal microscopy. J Histochem Cytochem 2005;53:1087–1097
8. Conrad E, Stein R, Hunter CS. Revealing transcription factors during human pancreatic β cell development. Trends Endocrinol Metab 2014;25:407–414
9. Dai C, Brissova M, Hang Y, et al. Islet-enriched gene expression and glucose-induced insulin secretion in human and mouse islets. Diabetologia 2012;55:707–718
10. Dai C, Kayton NS, Shostak A, et al. Stress-impaired transcription factor expression and insulin secretion in transplanted human islets. J Clin Invest 2016;126:1857–1870
11. Ji J, Petropavlovskaia M, Khatchadourian A, et al. Type 2 diabetes is associated with suppression of autophagy and lipid accumulation in β-cells. J Cell Mol Med 2019;23:2890–2900
12. Hunter CS, Stein RW. Evidence for loss in identity, de-differentiation, and *trans*-differentiation of islet β-cells in type 2 diabetes. Front Genet 2017;8:35
13. Spijker HS, Song H, Ellenbroek JH, et al. Loss of β-cell identity occurs in type 2 diabetes and is associated with islet amyloid deposits. Diabetes 2015;64:2928–2938
14. Andersson SA, Olsson AH, Esguerra JL, et al. Reduced insulin secretion correlates with decreased expression of exocytotic genes in pancreatic islets from patients with type 2 diabetes. Mol Cell Endocrinol 2012;364:36–45
15. Walker EM, Cha J, Tong X, et al. Sex-biased islet β cell dysfunction is caused by the MODY MAFA S64F variant by inducing premature aging and senescence in males. 6 January 2021 [preprint]. bioRxiv:2020.06.29.177527.
16. Scharfmann R, Pechberty S, Hazhouz Y, et al. Development of a conditionally immortalized human pancreatic β cell line. J Clin Invest 2014;124:2087–2098
17. Castaing M, Guerci A, Mallet J, Czernichow P, Ravassard P, Scharfmann R. Efficient restricted gene expression in beta cells by lentivirus-mediated gene transfer into pancreatic stem/progenitor cells. Diabetologia 2005;48:709–719
18. Wang X, McManus M. Lentivirus production. J Vis Exp 2009;(32):1499
19. Igoillo-Esteve M, Marselli L, Cunha DA, et al. Palmitate induces a pro-inflammatory response in human pancreatic islets that mimics CCL2 expression by beta cells in type 2 diabetes. Diabetologia 2010;53:1395–1405
20. Taneera J, Lang S, Sharma A, et al. A systems genetics approach identifies genes and pathways for type 2 diabetes in human islets. Cell Metab 2012;16:122–134
21. Pullen TJ, Khan AM, Barton G, Butcher SA, Sun G, Rutter GA. Identification of genes selectively disallowed in the pancreatic islet. Islets 2010;2:89–95
22. Fueger PT, Hernandez AM, Chen YC, Colvin ES. Assessing replication and beta cell function in adenovirally-transduced isolated rodent islets. J Vis Exp 2012;(64):4080
23. Kimmel AR, Sztalryd C. The perilipins: major cytosolic lipid droplet–associated proteins and their roles in cellular lipid storage, mobilization, and systemic homeostasis. Annu Rev Nutr 2016;36:471–509
24. Faleck DM, Ali K, Roat R, et al. Adipose differentiation-related protein regulates lipids and insulin in pancreatic islets. Am J Physiol Endocrinol Metab 2010;299:E249–E257
25. Plötz T, von Hanstein AS, Krümmel B, Laporte A, Mehmeti I, Lenzen S. Structure-toxicity relationships of saturated and unsaturated free fatty acids for elucidating the lipotoxic effects in human EndoC-βH1 beta-cells. Biochim Biophys Acta Mol Basis Dis 2019;1865:165525
26. Carr RM, Peralta G, Yin X, Ahima RS. Absence of perilipin 2 prevents hepatic steatosis, glucose intolerance and ceramide accumulation in alcohol-fed mice. PLoS One 2014;9:e97118
27. Osipovich AB, Stancill JS, Cartailler J-P, Dudek KD, Magnuson MA. Excitotoxicity and overnutrition additively impair metabolic function and identity of pancreatic β-cells. Diabetes 2020;69:1476–1491
28. Hattersley AT, Ashcroft FM. Activating mutations in Kir6.2 and neonatal diabetes: new clinical syndromes, new scientific insights, and new therapy. Diabetes 2005;54:2503–2513
29. Huang X, Wheeler MB, Kang YH, et al. Truncated SNAP-25 (1-197), like botulinum neurotoxin A, can inhibit insulin secretion from HIT-T15 insulinoma cells. Mol Endocrinol 1998;12:1060–1070
30. Pathomthongtaweechai N, Chutipongtanate S. AGE/RAGE signaling-mediated endoplasmic reticulum stress and future prospects in non-coding RNA therapeutics for diabetic nephropathy. Biomed Pharmacother 2020;131:110655
31. Gao Y, Zhang R, Dai S, Zhang X, Li X, Bai C. Role of TGF-β/Smad pathway in the transcription of pancreas-specific genes during beta cell differentiation. Front Cell Dev Biol 2019;7:351
32. Fonseca SG, Gromada J, Urano F. Endoplasmic reticulum stress and pancreatic β-cell death. Trends Endocrinol Metab 2011;22:266–274
33. Tong X, Kono T, Anderson-Baucum EK, et al. SERCA2 deficiency impairs pancreatic β-cell function in response to diet-induced obesity. Diabetes 2016;65:3039–3052
34. Talchai C, Xuan S, Lin HV, Sussel L, Accili D. Pancreatic β cell dedifferentiation as a mechanism of diabetic β cell failure. Cell 2012;150:1223–1234
35. Wong D. *Mapping Cellular Diversity and Lineage Dynamics Within the Developing Murine and Human Pancreas* (Doctoral dissertation, UCSF), 2019. San Francisco, CA, University of California, San Francisco
36. Zhang J, McKenna LB, Bogue CW, Kaestner KH. The diabetes gene Hhex maintains δ-cell differentiation and islet function. Genes Dev 2014;28:829–834
37. Chen E, Tsai TH, Li L, Saha P, Chan L, Chang BH. PLIN2 is a key regulator of the unfolded protein response and endoplasmic reticulum stress resolution in pancreatic β cells. Sci Rep 2017;7:40855
38. Butler PC, Meier JJ, Butler AE, Bhushan A. The replication of beta cells in normal physiology, in disease and for therapy. Nat Clin Pract Endocrinol Metab 2007;3:758–768
39. Tyrberg B, Andersson A, Borg LA. Species differences in susceptibility of transplanted and cultured pancreatic islets to the beta-cell toxin alloxan. Gen Comp Endocrinol 2001;122:238–251
40. Tsonkova VG, Sand FW, Wolf XA, et al. The EndoC-βH1 cell line is a valid model of human beta cells and applicable for screenings to identify novel drug target candidates. Mol Metab 2018;8:144–157
41. Mishra A, Liu S, Promes J, et al. Perilipin 2 downregulation in β cells impairs insulin secretion under nutritional stress and damages mitochondria. JCI Insight 2021;6:144341
42. Jarc E, Petan T. Lipid droplets and the management of cellular stress. Yale J Biol Med 2019;92:435–452
43. Chitraju C, Mejhert N, Haas JT, et al. Triglyceride synthesis by DGAT1 protects adipocytes from lipid-induced ER stress during lipolysis. Cell Metab 2017;26:407–418.e3
44. Wang C, Zhao Y, Gao X, et al. Perilipin 5 improves hepatic lipotoxicity by inhibiting lipolysis. Hepatology 2015;61:870–882
45. Bosma M, Dapito DH, Drosatos-Tampakaki Z, et al.; al. Sequestration of fatty acids in triglycerides prevents endoplasmic reticulum stress in an in vitro model of cardiomyocyte lipotoxicity. Biochim Biophys Acta 2014;1841:1648–1655
46. Harris L-ALS, Skinner JR, Shew TM, Pietka TA, Abumrad NA, Wolins NE. Perilipin 5-driven lipid droplet accumulation in skeletal muscle stimulates the expression of fibroblast growth factor 21. Diabetes 2015;64:2757–2768
47. Li Z, Liu H, Luo X. Lipid droplet and its implication in cancer progression. Am J Cancer Res. 2020;10:4112–4122

48. Ebrahimi AG, Hollister-Lock J, Sullivan BA, Tsuchida R, Bonner-Weir S, Weir GC. Beta cell identity changes with mild hyperglycemia: Implications for function, growth, and vulnerability. Mol Metab 2020; 35:100959

49. Libby AE, Bales ES, Monks J, Orlicky DJ, McManaman JL. Perilipin-2 deletion promotes carbohydrate-mediated browning of white adipose tissue at ambient temperature. J Lipid Res 2018;59:1482–1500

50. Guo S, Dai C, Guo M, et al. Inactivation of specific β cell transcription factors in type 2 diabetes. J Clin Invest 2013;123:3305–3316

51. Son J, Ding H, Accii D, Califano A. AFF3 and BACH2 are master regulators of metabolic inflexibility, β/α-cell transition, and dedifferentiation in type 2 diabetes. 12 September 2019 [preprint]. bioRxiv:768135

52. Lawlor N, George J, Bolisetty M, et al. Single-cell transcriptomes identify human islet cell signatures and reveal cell-type-specific expression changes in type 2 diabetes. Genome Res 2017;27:208–222

53. Poitout V, Robertson RP. Minireview: secondary beta-cell failure in type 2 diabetes–a convergence of glucotoxicity and lipotoxicity. Endocrinology 2002; 143:339–342

54. Ahmadian M, Suh JM, Hah N, et al. PPARγ signaling and metabolism: the good, the bad and the future. Nat Med 2013;19:557–566

55. Mihalik SJ, Michaliszyn SF, de las Heras J, et al. Metabolomic profiling of fatty acid and amino acid metabolism in youth with obesity and type 2 diabetes: evidence for enhanced mitochondrial oxidation. Diabetes Care 2012;35: 605–611

56. Krahmer N, Najafi B, Schueder F, et al. Organellar proteomics and phospho-proteomics reveal subcellular reorganization in diet-induced hepatic steatosis. Dev Cell 2018;47:205–221.e7

57. Najt CP, Mashek DG. The lipid droplet as a signaliTFMng node. In *Lipid Signaling and Metabolism*. Ntambi JM, Ed. Cambridge, MA, Elsevier, 2020, pp. 157–172